A noise robust method based on completed local binary patterns for hot-rolled steel strip surface defects

Kechen Song*, Yunhui Yan

School of Mechanical Engineering & Automation, Northeastern University, Shenyang, Liaoning 110819, PR China

A B S T R A C T

Automatic recognition method for hot-rolled steel strip surface defects is important to the steel surface inspection system. In order to improve the recognition rate, a new, simple, yet robust feature descriptor against noise named the adjacent evaluation completed local binary patterns (AECLBPs) is proposed for defect recognition. In the proposed approach, an adjacent evaluation window which is around the neighbor is constructed to modify the threshold scheme of the completed local binary pattern (CLBP). Experimental results demonstrate that the proposed approach presents the performance of defect recognition under the influence of the feature variations of the intra-class changes, the illumination and grayscale changes. Even in the toughest situation with additive Gaussian noise, the AECLBP can still achieve the moderate recognition accuracy. In addition, the strategy of using adjacent evaluation window can also be used in other methods of local binary pattern (LBP) variants.

© 2013 Elsevier B.V. All rights reserved.

1. Introduction

Steel strip is one of the main products of iron and steel industry, and its quality directly affects the quality and performance of the final product. Meanwhile, the quality of the steel strip is related to the economic benefits of iron and steel enterprises and has become one of the key indicators of iron and steel market competition. Due to the limitations of production conditions, the surface of the steel strip inevitably exist different types of defects, e.g., scratches, surface crazing and rolled-in scale. These defects not only affect the appearance of the product, but also reduce the properties of the product such as corrosion resistance, abrasion resistance and fatigue strength, which can cause huge economic losses to the enterprise. Therefore, real-time accurate inspection of surface defects has become an indispensable section in the iron and steel enterprises.

In the early 1990s, the traditional methods of the surface inspection mainly include: artificial visual inspection, magnetic flux leakage testing [1], etc. Due to the influence of the subjective factor and high error inspection rate, these methods cannot meet the requirement of real-time [2]. In recent years, the visual-based inspection technology, as a kind of non-contact inspection method, has become a research hotspot in the field of surface defects inspection. This method integrates many advanced technologies including image processing, optics, pattern recognition,

artificial intelligence, hence it has obtained real-time, high accuracy rate and reliability. In view of the characteristics of the real-time and easy to realize intelligently, this technology has been widely used in the online real-time inspection of the automatic production lines such as paper [3], glass [4], and steel bar [5].

The automated surface inspection system of the steel mainly includes two components: rapid detection and defect recognition. The first component is for the purpose of acquiring defect images and locating the positions of the defects. In this component, defect images can be acquired with varied methods, for instance, multiple-curvature [6] and multi-modal [7]. The positions of the defects then can be located with various methods including interactive evolution [8], engineering-driven rule-based detection (ERD) [9], undecimated wavelet transform [10], univariate dynamic encoding algorithm for searches (uDEAS) [11], clustering algorithm [12], and morphology [13]. In the second component, the defect features can be extracted with varied methods such as gabor filters [14], wavelet filters [15], and multi-scale geometric analysis (MGA) [16]. Then the extracted features can be classified by diversified classifiers, e.g., Bayesian network [17], support vector machine (SVM) [18], and process knowledge based support vector (PK-MSVM) [19].

At present, the main task of the steel surface inspection system is to improve the recognition rate. Despite the several methods mentioned above have achieved moderate results by means of improved features and classifier, there are three difficult challenges to overcome. These challenges are as follows:

1. The intra-class defects existing large differences in appearance while the inter-class defects have similar aspects, i.e., the

---

* Corresponding author. Tel.: +86 24 83678545.
  E-mail address: unkechen@gmail.com (K. Song).

features of the intra-class defects are too scattered while the features of the inter-class defects are too similar. The further illustrations of this challenge are presented in Section 4.2.

2. Due to the influence of the illumination and material changes, the gray values of the acquired defect images can be easily changed. The changed gray values then will affect the stability of the extracted defect features. Hence, the unstable features will lower the recognition rate.

3. Most of the employed features are vulnerable to noise, which include the local binary pattern (LBP) feature [20], wavelet feature and MGA feature. The sensitivity to noise reduces the stability of the features.

All of these challenges affect the stability of the extracted defect features from different aspects. However, most of the methods of feature extraction only take one or two of the challenges into account. For example, wavelet feature [15] and MGA feature [16] are sensitive to noise, i.e., these features encounter the third challenge. Therefore, to solve the three issues mentioned above is indeed a difficult challenge. In order to resolve the first two difficult challenges, we investigate the local binary pattern (LBP) [20] which has been known as one of the most successful statistical approaches for texture classification due to its gray-scale and rotation invariance. Although the LBP and the completed local binary pattern (CLBP) [21] have achieved the great success in the feature classification, their threshold schemes are sensitive to noise, i.e., they suffer from the third difficult challenge. In order to overcome this problem, an adjacent evaluation window which is around the neighbor is constructed to modify the threshold scheme of CLBP. Moreover, experimental results demonstrate that the strategy of using adjacent evaluation window plays an important role in solving the issue of sensitivity to noise in CLBP.

The rest of this paper is organized as follows: Section 2 presents the structure of the automated surface inspection system procedures. Section 3 introduces the proposed noise robust automatic recognition method in detail. Then Section 4 elaborates the experiments and discusses the experimental results. Finally, Section 5 concludes the paper.

2. Structure of automated surface inspection system

The structure of the automated surface inspection system is shown in Fig. 1. This system is installed after laminar cooling. After laminar cooling, the temperature of the surface ranges from 500 °C to 700 °C. According to the required thickness of the hot-rolled steel strip, the rolling speed of the steel strip varies from a minimum of 3 m/s to the maximum capacity of the mill of 18 m/s, the width of steel strip varies from 1580 mm to 2160 mm. The system mainly consists of four subsystems: image acquisition, rapid detection, feature extraction, and defect classification.

2.1. Image acquisition subsystem

The hardware configuration of the image acquisition mainly includes two components: light source and cameras. The light source provides illumination to make the defects visible. Since the light-emitting diode (LED) has many advantages such as little power and longevity, it is used to produce the narrow-spectrum light in this work. In order to cover the width of the steel strip, four area scan CCD cameras are used. The size of original grayscale images is 1024×1024 pixels. In this work, in order to save calculation time for subsequent sections, the original images are performed on down sampling process, i.e., the sampled images are set as 200×200 pixels.

2.2. Rapid detection subsystem

In this subsystem, the defect-free images are promptly deleted for the purpose of saving memory space. Moreover, the positions of the defects are rapidly located for the requirement of the feature extraction and defect classification. In order to promptly pinpoint the defects and delete the defect-free images, this subsystem must satisfy the properties of real-time, veracity and reliability. In this work, the gray projection algorithm, as one of the methods of low-time consumption, is applied to detect and delete the defect-free images. Then, the area search method is employed to locate the positions of the defects rapidly.

2.3. Feature extraction subsystem

The feature extraction subsystem, as one of the important tasks of surface inspection system, is mainly to describe the defect characteristics. Since the intra-class defects existing large variations in appearance such as size and orientation, the extracted features need to satisfy the invariance of size and rotation. Meanwhile, the stability of the features needs to meet the requirement of the subsystem. Although varied methods have been employed to extract the defect features including gabor filters, wavelet filters, and MGA, there still remain several difficult challenges (i.e., those mentioned in Section 1) to overcome. Therefore, this work proposes a new method to address these challenges, i.e., the adjacent evaluation completed local binary patterns (AECLBPs).
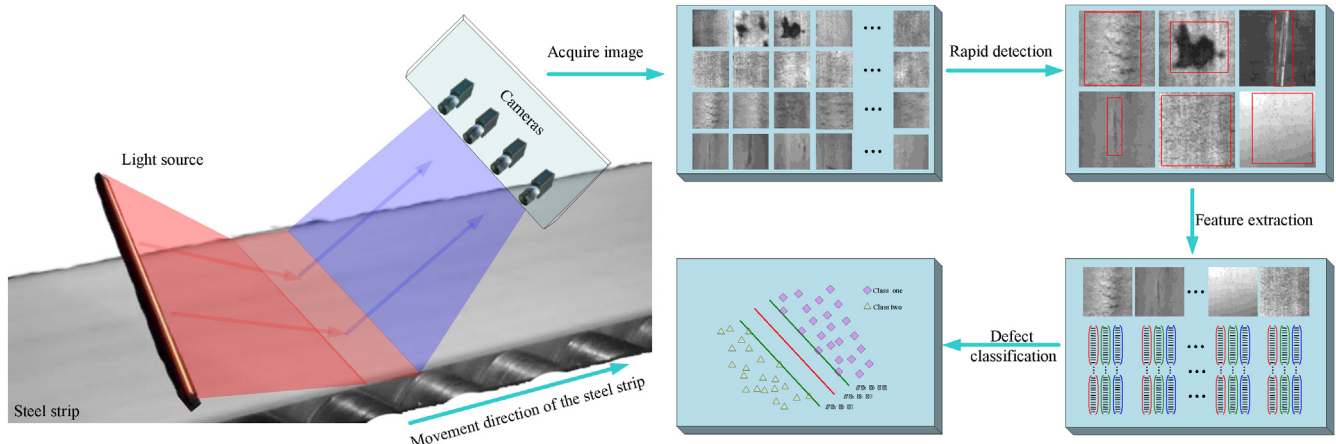

Fig. 1. Structure of automated surface inspection system.

2.4. Defect classification subsystem

In this subsystem, the extracted features are attached class labels by means of a classifier. However, the classification accuracy of the classifier mainly depends on the performance of the features and the training dataset. Therefore, linearly separable features and ample training dataset will improve the performance of the classifier. Currently, diversified classifiers have been employed to classify the defect features, which include Bayesian network, SVM, PK-MSVM, and nearest neighbor classifier (NNC). In this work, in order to evaluate the proposed feature method, the commonly applied classifiers are employed, i.e., SVM and NNC.

3. Noise robust automatic recognition method

In this section, to improve the recognition rate of the steel surface inspection system, a new feature descriptor against noise named the AECLBP is proposed for defect recognition.

3.1. AECLBP-based feature extraction

In the conventional CLBP operator, local binary codes are extracted by comparing the values of neighborhood pixels with the value of the central pixel and then are encoded to form the local binary patterns. However, this conventional encoding strategy is especially vulnerable to noise, i.e., the values of the neighbors can be very easily changed by random noise, making the local binary patterns unstable. Concerning this issue, we try to construct an adjacent evaluation window which is around the neighbor to reduce the interference of noise. Moreover, inspired by the encoded strategy of CLBP, we propose an approach named the AECLBP, which can be considered as an extension of CLBP.

As is operated with the CLBP, the image local differences of the AECLBP are decomposed into two complementary components: the sign (s_p) and the magnitude (m_p). The s_p and m_p are described as:

$$s_p = s(a_p - g_c), \quad m_p = |a_p - g_c| \tag{1}$$

where g_c is the grayscale value at central point, a_p is set as the average value of the pth evaluation window excluding the value
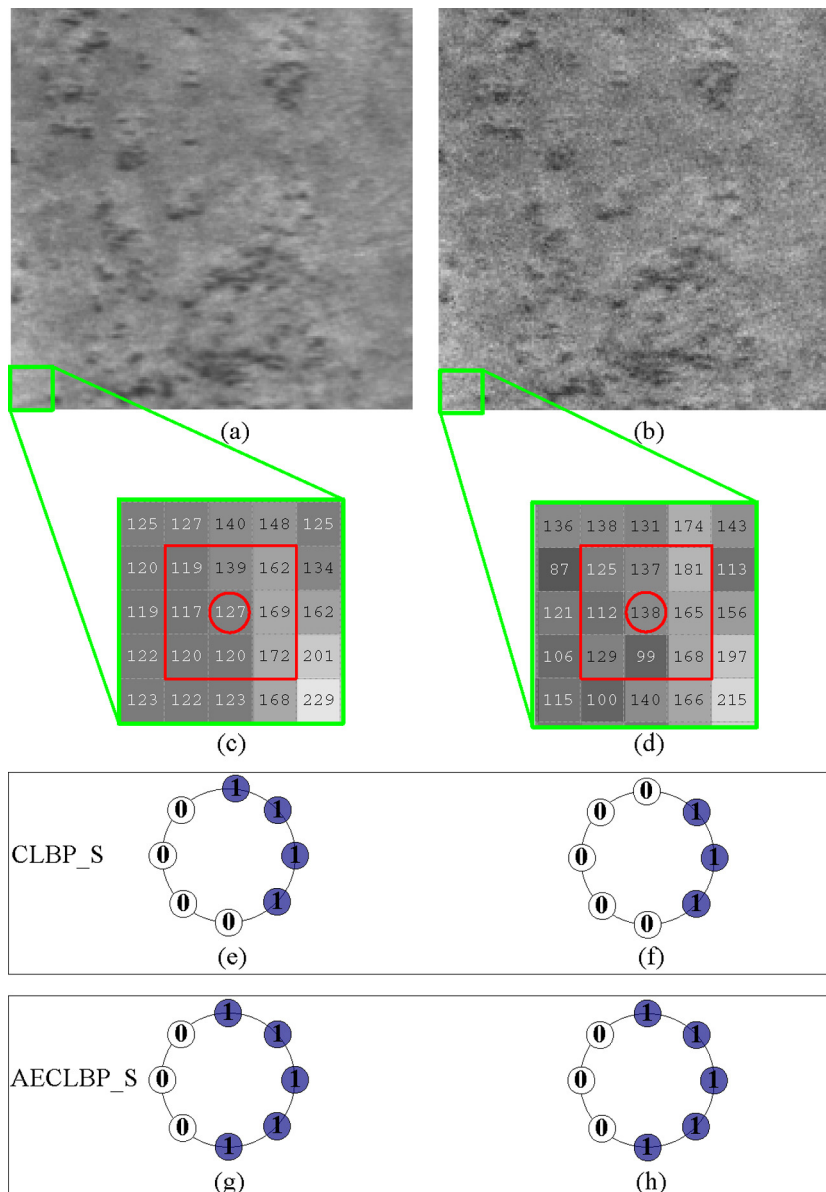

Fig. 2. Comparison of the robustness to additive Gaussian noise (SNR = 20 dB) between the proposed AECLBP and the CLBP on the defect image (rolled-in scale).

of evaluation center. Then two operators, AECLBP-Sign (AECLBP_S) and AECLBP-Magnitude (AECLBP_M), are proposed to code them. The AECLBP_S is defined as follows:

$$AECLBP\_S_{P,R} = \sum_{p=0}^{P-1} s(a_p - g_c)2^p, \quad s(x) = \begin{cases} 1 & x \geq 0 \\ 0 & x < 0 \end{cases} \tag{2}$$

where P points spaced equidistantly around a circle of radius R, g_c and a_p are defined in Eq. (1). The AECLBP_M is defined as:

$$AECLBP\_M_{P,R} = \sum_{p=0}^{P-1} t(m_p, c)2^p, \quad t(x, c) = \begin{cases} 1, & x \geq c \\ 0, & x < c \end{cases} \tag{3}$$

where m_p is defined in Eq. (1), and the threshold c is set as the mean value of m_p of the whole image. Moreover, the AECLBP_C is defined identical to the CLBP_C. Inspired by the combined way of CLBP, these operators (AECLBP_S, AECLBP_M, and AECLBP_C) are combined, i.e., AECLBP_S/M/C.

Obviously, the main difference between the CLBP and the AECLBP is that AECLBP replaces the g_p with a_p. The entire operation procedure of the AECLBP mainly includes the following two steps:

(1) *Calculating the value of a_p*. Set the neighbor which is around the neighborhood center g_c as the evaluation center a_p. Surrounding the evaluation center, we set up an evaluation window of size $W \times W$ (W can only be odd numbers). Then, excluding the pixel value of the evaluation center, the value of a_p is obtained by calculating the average of the remaining values in the pth evaluation window. What needs to be noted is that when the value of W is set as 1, AECLBP is equivalent to the CLBP.

(2) *Forming the local binary patterns*. Local binary codes are extracted by comparing the value of a_p with the value of the neighborhood center g_c. Then, the local binary codes are encoded to form the patterns.

To illustrate the effectiveness of AECLBP, Fig. 2 gives a comparison of the robustness to additive Gaussian noise (SNR = 20 dB) between the proposed AECLBP (W is set as 3) and the CLBP on the defect image (rolled-in scale). The original defect image is shown in Fig. 2(a) and the corresponding image with additive Gaussian noise is shown in Fig. 2(b). For the pixel region of size 5 × 5, Fig. 2(c) and (d), are extracted from the same location (i.e. bottom left) of the corresponding image, respectively. The patterns of CLBP_S for corresponding pixel region, Fig. 2(e) and (f), are obtained. Meanwhile, the patterns of AECLBP_S are given in Fig. 2(g) and (h).

From Fig. 2, we can clearly observe that the pattern value of CLBP_S is changed since the Gaussian noise is added to the corresponding pixel region. Fig. 3 shows the nine rotation invariant "uniform" patterns in $CLBP\_S_{8,R}^{riu2}$, in which the numbers inside them correspond to their unique codes. According to Fig. 3, the pattern

value of CLBP_S is changed from 4 into 5 because of the interference of noise. By contrast, the pattern value of AECLBP_S maintains at 3, i.e., the pattern value of AECLBP_S does not change under the interference of noise.

3.2. Multi-scale analysis and classification

To make the representation more robust, the coarse and fine information of the features can be captured by multi-scale. In this study, we combine the information obtained by multiple descriptors of varying (P, R). The histogram feature vector of multi-scale analysis is obtained by concatenating the histograms from a single scale analysis realized with different (P, R).

To classify the extracted features of defects, the nearest neighbor classifier (NNC) and the support vector machine (SVM) are used to assign the defect class. In the nearest neighbor classifier, the chi-square distance is used, which is defined as:

$$D(H, K) = \sum_{i=1}^{B} \frac{(h_i - k_i)^2}{h_i + k_i} \tag{4}$$

where $H = \{h_i\}$ and $K = \{k_i\}(i = 1, 2 \ldots, B)$ denote two histograms.

4. Experimental results and discussion

To demonstrate the effectiveness of the proposed approach for defect recognition, a surface defect database is used, which is described in detail in the following section. Meanwhile, the proposed approach is compared with other approaches on the surface defect database. In addition, the robustness of the proposed approach against the interference of noise is examined.

4.1. Compared methods and implementation details

The recognition rate of the proposed approach has been compared with other approaches such as LBP [20], local ternary patterns (LTP) [22], and CLBP [21]. In this work, the rotation invariant uniform patterns are used under multi-scale scheme, i.e., $LBP_{8,1+16,2+24,3}^{riu2}$, $LTP_{8,1+16,2+24,3}^{riu2}$, and $CLBP\_S_{8,1+16,2+24,3}^{riu2}/M_{8,1+16,2+24,3}^{riu2}/C$.

Implementation details: Analogous to the work presented in [20] and [21], each defect sample of the proposed approach is normalized to have an average intensity of 128 and a standard deviation of 20. The size of evaluation window for the proposed approaches is set as 3 × 3 and the user-specified threshold t of LTP is set as 5. The LIBSVM toolbox [23] for the implementation of SVM classifier is used here. The radial basis function (RBF) is selected as the kernel function. The parameters of the classifier are determined by the cross-validation testing. Furthermore, 150 samples per class are randomly elected for training and the remaining for testing. To
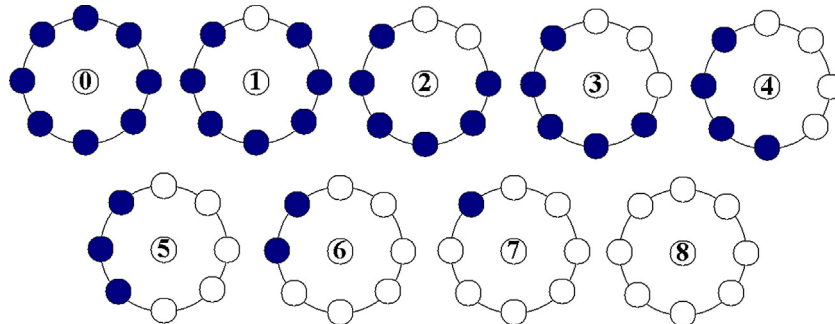

Fig. 3. The nine rotation invariant "uniform" patterns and the numbers inside them correspond to their unique $LBP_{8,R}^{riu2}$ codes.
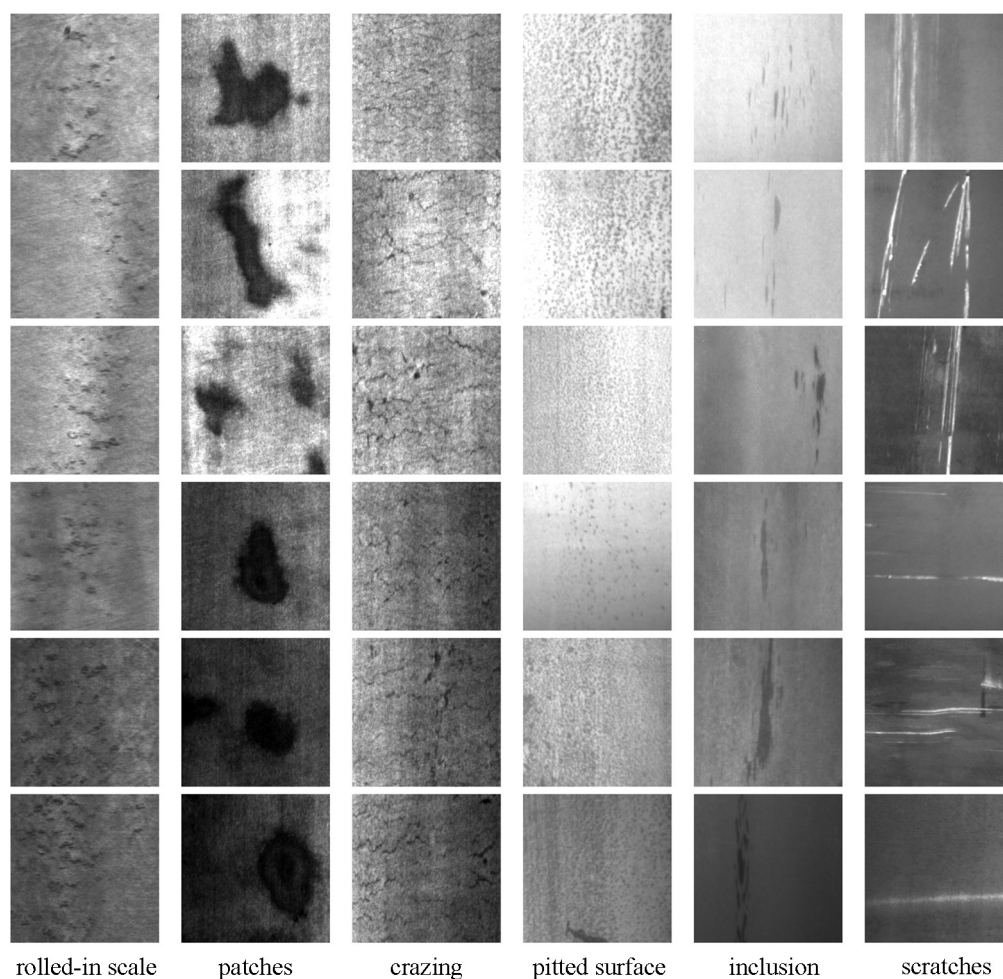
Fig. 4. Samples of six kinds of typical surface defects on NEU surface defect database. Each row shows one example image from each of 300 samples of a class.

evaluate the robustness against additive Gaussian noise for the proposed approach, defect images without noise serves as training set, but each defect sample of testing set is added Gaussian noise with different signal-to-noise ratios (SNR = 50 dB, 40 dB, 30 dB, 20 dB). All the results of the proposed approach are reported over a hundred random partitions of training and testing sets. Then the average classification accuracy and the standard deviations are calculated for each database.

4.2. NEU surface defect database

In order to demonstrate the effectiveness of the proposed approach for defect recognition, a surface defect database named the Northeastern University (NEU) surface defect database is constructed. In this database, six kinds of typical surface defects of the hot-rolled steel strip are collected, i.e., rolled-in scale (RS), patches (Pa), crazing (Cr), pitted surface (PS), inclusion (In) and scratches (Sc). The database includes 1800 grayscale images: 300 samples each of six different kinds of typical surface defects. Fig. 4 shows the sample images of six kinds of typical surface defects, the original resolution of each image is 200 × 200. In this work, the same kind of defects is defined as the "intra-class defects", while the different classes of defects are defined as the "inter-class defects". For example, in Fig. 4, the same columns of the defects belong to the "intra-class defects", while the different columns of the defects belong to the "inter-class defects". From Fig. 4, we can clearly observe that the intra-class defects existing large differences in appearance, for instance, the scratches (the last column) may be horizontal scratch,

vertical scratch, and slanting scratch, etc. Meanwhile the inter-class defects have similar aspects, e.g., rolled-in scale, crazing, and pitted surface. In addition, due to the influence of the illumination and material changes, the grayscale of the intra-class defect images is varied. In short, the NEU surface defect database includes the first two difficult challenges mentioned in Section 1.

The average recognition accuracy and the standard deviations on NEU surface defect database are shown in Table 1. From the produced results, it is observed that the proposed AECLBP approach achieves the best average recognition accuracy (98.93%) in the methods of comparison. Moreover, in the experimental results of the proposed approach, it is observed that the performance of SVM classifier is slightly better than that of the NNC. Additionally, these results demonstrate the performance of the proposed approach even in the difficult challenges.

Table 1
The recognition accuracy (%) on the NEU surface defect database.

Method	Classifier	Accuracy
LBP	NNC	95.07 ± 0.71
	SVM	97.93 ± 0.66
LTP	NNC	95.93 ± 0.39
	SVM	98.22 ± 0.52
CLBP	NNC	96.91 ± 0.24
	SVM	98.28 ± 0.51
AECLBP	NNC	97.93 ± 0.21
	SVM	$\mathbf{98.93 \pm 0.63}$

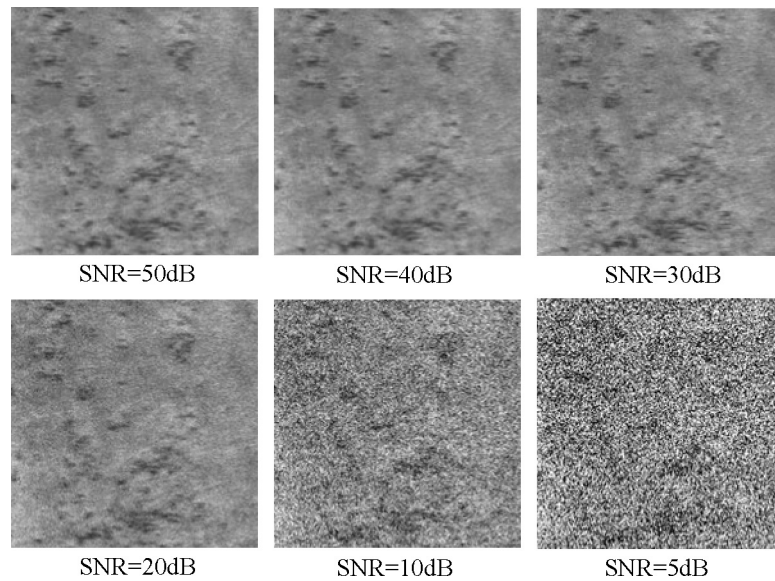The bold value presents the best result in all of the results.

Fig. 5. Surface defect images polluted by Gaussian noise with different SNR.

In order to investigate the recognition results for six different kinds of typical surface defects in detail, the confusion matrix of the proposed approach on the NEU surface defect database is shown in Table 2. In this experiment, 150 defect samples of each class are randomly elected for testing and the NNC is used here. From Table 2, we can observe that the RS defects achieve the best result (the recognition accuracy is 100%). Although the total recognition accuracy of the approach is 97.89%, the experimental results of the PS defects and In defects are slightly worse than that of the other kinds of defects.

4.3. Robustness to noise

In order to objectively evaluate the robustness against additive Gaussian noise for the proposed approach, noisy defect images are conducted. In this experiment, defect images without noise serves as training set, but each defect sample of testing set is added Gaussian noise with different SNR value. Fig. 5 shows some defect images polluted by Gaussian noise with different SNR. From this figure, we can observe that the defects are almost covered by noise when the SNR value drops below 20 dB. As the matter of fact, this situation (i.e. the SNR value drops below 20 dB) rarely appears. In view of the practical condition, four different SNR values (i.e. 50 dB, 40 dB, 30 dB, and 20 dB) are adopted in our experiments. To reduce the variability of randomness, each experiment is repeated a hundred times randomly. Then the average classification accuracy and the standard deviations are presented in Table 3.

As we can see in Table 3, except for the LBP, all other methods maintain their performance on the database when SNR ≥ 40 dB. However, when the SNR value drops below 40 dB, the noise rises so that different methods have considerable declines of accuracy. It can also observe that the proposed method consistently

outperformed all the other methods in comparison with different SNR. Even in the toughest situation (SNR = 20 dB), the AECLBP achieves the moderate recognition accuracy. In addition, the performance of SVM classifier is slightly better than that of the NNC.

4.4. Discussion

On the whole, the proposed approach presents the performance of defect recognition under the influence of the feature variations of the intra-class changes, the illumination and grayscale changes. Even in the toughest situation with additive Gaussian noise, the AECLBP can still achieve the moderate recognition accuracy. Moreover, these results demonstrate that the strategy of using adjacent evaluation window plays an important role in solving the issue of sensitivity to noise in CLBP.

Furthermore, Fig. 6 shows the relationship between the recognition accuracy of different methods and the number of the training test for each class under the interference of noise (SNR = 30 dB). It is revealed that the AECLBP, CLBP, and LBP achieve the same recognition accuracy when the number is 90 and 150. Therefore, the number of the training test for each class can be set as 90 in the future experiments. In addition, we also investigated the recognition accuracy of evaluation window of different sizes (e.g. 3×3, 5×5, 7×7, 9×9) on the NEU surface defect database. We found

Table 2
The confusion matrix of the proposed method on the NEU surface defect database.

	RS	Pa	Cr	PS	In	Sc
RS	150	0	0	0	0	0
Pa	0	147	3	0	0	0
Cr	0	1	149	0	0	0
PS	0	3	2	144	1	0
In	2	1	1	1	144	1
Sc	0	0	0	0	3	147

Fig. 6. The recognition accuracy (%) with different number of the training test for each class (SNR = 30 dB).

Table 3
The recognition accuracy (%) with different Gaussian noise on the NEU surface defect database.

Method	Classifier	SNR = 50 dB	SNR = 40 dB	SNR = 30 dB	SNR = 20 dB
LBP	NNC	67.93 ± 0.59	65.02 ± 1.76	57.93 ± 1.86	20.60 ± 4.79
	SVM	73.87 ± 0.49	69.56 ± 0.99	62.36 ± 2.85	22.53 ± 3.96
LTP	NNC	95.56 ± 0.85	92.11 ± 1.37	58.91 ± 1.88	18.60 ± 1.06
	SVM	98.18 ± 0.42	97.60 ± 0.69	67.62 ± 2.23	24.98 ± 5.94
CLBP	NNC	94.40 ± 0.46	90.07 ± 1.41	73.09 ± 0.94	23.04 ± 1.33
	SVM	98.11 ± 0.39	97.04 ± 0.67	74.84 ± 1.03	27.42 ± 3.25
AECLBP	NNC	97.87 ± 0.48	96.38 ± 0.69	79.69 ± 1.32	31.20 ± 3.46
	SVM	**98.87 ± 0.37**	**98.53 ± 0.39**	**88.29 ± 1.70**	**37.09 ± 2.15**

The bold value presents the best result in all of the results.

that the best recognition accuracy was obtained when the size of the evaluation window was set as 3×3. In texture classification, it is often believed that various extension methods of the LBP can characterize the local texture effectively by detecting the "micro-structure". However, larger evaluation windows are not beneficial to extracting the information of the "micro-structure". Therefore, the 3×3 evaluation window obtained better recognition accuracy than the other windows.

5. Conclusion

Since the main task of the steel surface inspection system is to improve the recognition rate, a new, simple, yet robust feature descriptor against noise named the AECLBP is proposed for defect recognition. An adjacent evaluation window which is around the neighbor is constructed to improve the interference of noise. The proposed approach not only presents the performance of defect recognition under the influence of the feature variations of the intra-class changes on the NEU surface defect database, but also achieves the moderate recognition accuracy in the toughest situation with additive Gaussian noise. In a word, the strategy of using adjacent evaluation window plays an important role in solving the issue of sensitivity to noise in CLBP. Besides, the strategy can also be used in other methods of LBP variants (e.g. CLBC). Since the number of defect categories of the NEU surface defect database is relatively small, the future work includes the extension of the defect category. Meanwhile, more research on advanced classifiers will be conducted to further improve the performance of the defect recognition.

Acknowledgment

References

[1] H. Maki, Y. Tsunozaki, Y. Matsufuji, Magnetic on-line defect inspection system for strip steel, Iron and Steel Engineer 70 (1993) 56–59.
[2] X. Li, S.K. Tso, X.P. Guan, Q. Huang, Improving automatic detection of defects in castings by applying wavelet technique, IEEE Transactions on Industrial Electronics 53 (2006) 1927–1934.
[3] A. Alam, J. Thim, M. O'Nils, A. Manuilskiy, J. Lindgren, J. Lidén, Online surface characterization of paper and paperboards in a wide-range of the spatial wavelength spectrum, Applied Surface Science 258 (2012) 7928–7935.
[4] S.M. Chao, D.M. Tsai, An anisotropic diffusion-based defect detection for low-contrast glass substrates, Image and Vision Computing 26 (2008) 187–200.
[5] W.B. Li, C.H. Lu, J.C. Zhang, A local annular contrast based real-time inspection algorithm for steel bar surface defects, Applied Surface Science 258 (2012) 6080–6086.
[6] G. Rosati, G. Boschetti, A. Biondi, A. Rossi, Real-time defect detection on highly reflective curved surfaces, Optics and Lasers in Engineering 47 (2009) 379–384.
[7] D. Martin, D.M. Guinea, M.C. García-Alegre, E. Villanueva, D. Guinea, Multi-modal defect detection of residual oxide scale on a cold stainless steel strip, Machine Vision and Applications 21 (2010) 653–666.
[8] P. Caleb-Solly, J.E. Smith, Adaptive surface inspection via interactive evolution, Image and Vision Computing 25 (2007) 1058–1072.
[9] E. Pan, L. Ye, J.J. Shi, T.S. Chang, On-line bleeds detection in continuous casting processes using engineering-driven rule-based algorithm, Journal of Manufacturing Science and Engineering 131 (2009) 061008–61011.
[10] J.P. Yun, S.H. Choi, S.W. Kim, Vision-based defect detection of scale-covered steel billet surfaces, Optical Engineering 48 (2009) 037205–37211.
[11] J.P. Yun, S.H. Choi, J.W. Kim, S.W. Kim, Automatic detection of cracks in raw steel block using Gabor filter optimized by univariate dynamic encoding algorithm for searches (uDEAS), NDT & E International 42 (2009) 389–397.
[12] F.G. Bulnes, R. Usamentiaga, D.F. García, J. Molleda, Vision-based sensor for early detection of periodical defects in web materials, Sensors 12 (2012) 10788–10809.
[13] A. Landström, M.J. Thurley, Morphology-based crack detection for steel slabs, IEEE Journal of Selected Topics in Signal Processing 6 (2012) 866–875.
[14] R. Medina, F. Gayubo, L.M. González-Rodrigo, et al., Automated visual classification of frequent defects in flat steel coils, International Journal of Advanced Manufacturing Technology 57 (2011) 1087–1097.
[15] S. Ghorai, A. Mukherjee, M. Gangadaran, P.K. Dutta, Automatic defect detection on hot-rolled flat steel products, IEEE Transactions on Instrumentation and Measurement 62 (2013) 612–621.
[16] K. Xu, Y.H. Ai, X.Y. Wu, Application of multi-scale feature extraction to surface defect classification of hot-rolled steels, International Journal of Minerals, Metallurgy, and Materials 20 (2013) 37–41.
[17] F. Pernkopf, Detection of surface defects on raw steel blocks using Bayesian network classifiers, Pattern Analysis and Applications 7 (2004) 333–342.
[18] X.W. Zhang, Y.Q. Ding, Y.Y. Lv, et al., A vision inspection system for the surface defects of strongly reflected metal based on multi-class SVM, Expert Systems with Applications 38 (2011) 5930–5939.
[19] K. Agarwal, R. Shivpuri, Y. Zhu, T.S. Chang, H. Huang, Process knowledge based multi-class support vector classification (PK-MSVM) approach for surface defects in hot rolling, Expert Systems with Applications 38 (2011) 7251–7262.
[20] T. Ojala, M. Pietikäinen, T. Mäenpää, Multiresolution gray-scale and rotation invariant texture classification with local binary patterns, IEEE Transactions on Pattern Analysis and Machine Intelligence 24 (2002) 971–987.
[21] Z.H. Guo, L. Zhang, D. Zhang, A completed modeling of local binary pattern operator for texture classification, IEEE Transactions on Image Processing 19 (2010) 1657–1663.
[22] X.Y. Tan, B. Triggs, Enhanced local texture feature sets for face recognition under difficult lighting conditions, IEEE Transactions on Image Processing 19 (2010) 1635–1650.
[23] C.C. Chang, C.J. Lin, LIBSVM: A Library for Support Vector Machines, Software available from http://www.csie.ntu.edu.tw/~cjlin/libsvm, 2001.